

MGH: Metadata Guided Hypergraph Modeling for Unsupervised Person Re-identification

Yiming Wu
Zhejiang University
Hangzhou, Zhejiang, China
yimingwu0@gmail.com

Xi Li*
Zhejiang University
Hangzhou, Zhejiang, China
xilizju@zju.edu.cn

Xintian Wu
Zhejiang University
Hangzhou, Zhejiang, China
hsintien@zju.edu.cn

Jian Tian
Zhejiang University
Hangzhou, Zhejiang, China
tianjian29@zju.edu.cn

ABSTRACT

As a challenging task, unsupervised person ReID aims to match the same identity with query images which does not require any labeled information. In general, most existing approaches focus on the visual cues only, leaving potentially valuable auxiliary metadata information (e.g., spatio-temporal context) unexplored. In the real world, such metadata is normally available alongside captured images, and thus plays an important role in separating several hard ReID matches. With this motivation in mind, we propose **MGH**, a novel unsupervised person ReID approach that uses meta information to construct a hypergraph for feature learning and label refinement. In principle, the hypergraph is composed of camera-topology-aware hyperedges, which can model the heterogeneous data correlations across cameras. Taking advantage of label propagation on the hypergraph, the proposed approach is able to effectively refine the ReID results, such as correcting the wrong labels or smoothing the noisy labels. Given the refined results, We further present a memory-based listwise loss to directly optimize the average precision in an approximate manner. Extensive experiments on three benchmarks demonstrate the effectiveness of the proposed approach against the state-of-the-art.

CCS CONCEPTS

• Information systems → Image search.

KEYWORDS

Unsupervised Person Re-Identification; Metadata; Hypergraph; Listwise Loss; Memory

ACM Reference Format:

Yiming Wu, Xintian Wu, Xi Li, and Jian Tian. 2021. MGH: Metadata Guided Hypergraph Modeling for Unsupervised Person Re-identification. In *Proceedings of the 29th ACM International Conference on Multimedia (MM '21)*, October 20–24, 2021, Virtual Event, China.

*Corresponding author

Permission to make digital or hard copies of all or part of this work for personal or classroom use is granted without fee provided that copies are not made or distributed for profit or commercial advantage and that copies bear this notice and the full citation on the first page. Copyrights for components of this work owned by others than the author(s) must be honored. Abstracting with credit is permitted. To copy otherwise, or republish, to post on servers or to redistribute to lists, requires prior specific permission and/or a fee. Request permissions from permissions@acm.org.

MM '21, October 20–24, 2021, Virtual Event, China

© 2021 Copyright held by the owner/author(s). Publication rights licensed to ACM.
ACM ISBN 978-1-4503-8651-7/21/10...\$15.00
<https://doi.org/10.1145/3474085.3475296>

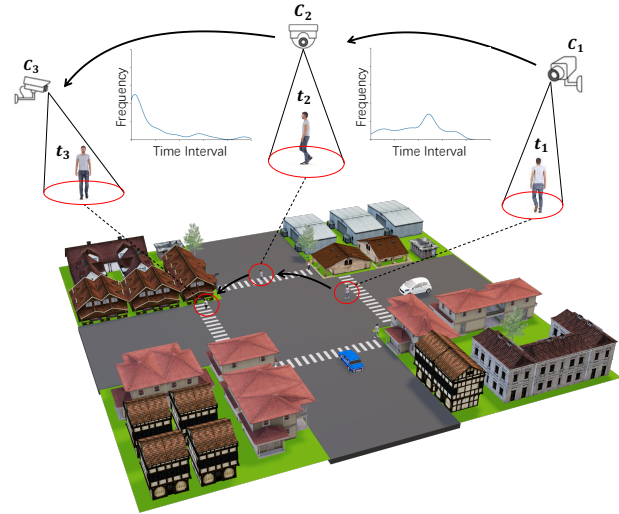


Figure 1: Illustration of the distributed camera network. The metadata (i.e. camera index, timestamp, etc.) is valuable to distinguish as well as associate persons of interest. Camera information is helpful to guide the learning of camera-invariance feature representation. Camera-timestamp tuples could be used to measure the transition probability with a prior spatio-temporal distribution.

October 20–24, 2021, Virtual Event, China. ACM, New York, NY, USA, 10 pages.
<https://doi.org/10.1145/3474085.3475296>

1 INTRODUCTION

Given a person of interest for query, person re-identification(ReID) aims to search the same identities against gallery, it has been widely used in many real-world applications, such as video surveillance system, robotics, human-computer interaction, etc. Due to the expensive annotation cost, recent researches focus on the unsupervised person ReID, which requires no manual annotations. Moreover, ReID is generally carried out in a distributed camera network, where a wealth of auxiliary metadata (e.g. camera index, timestamp, etc.) is attached with the captured images. As shown in Figure 1, the metadata could provide auxiliary guidance to unsupervised person ReID [23, 24, 31, 33, 40, 43, 49, 51, 66, 68], but how to adequately

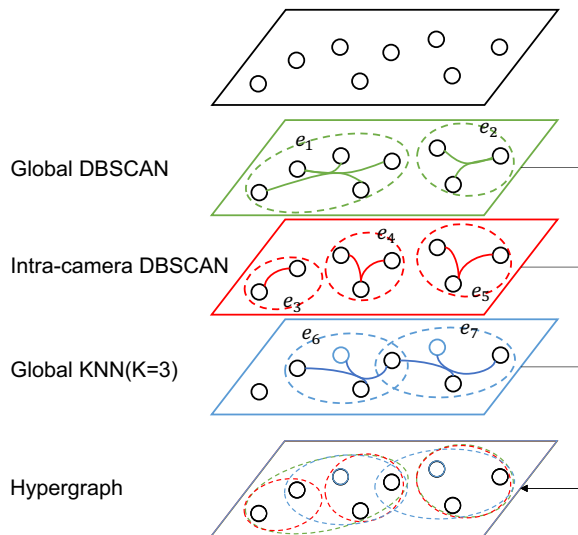


Figure 2: Illustration of hypergraph construction. We investigate different hyperedge construction strategies, i.e. KNN, clustering, camera-aware clustering. **Global Clustering:** perform global clustering and group the instances in a cluster as a hyperedge. **Intra-camera Clustering:** camera information is combined with clustering to perform intra-camera Clustering. **Global KNN:** given a vertex (i.e., centroid), a hyperedge connects itself and its nearest neighbors.

utilize such heterogeneous structure in unsupervised ReID is still an open problem.

Recently, unsupervised person ReID approaches [9, 12, 60] follow clustering-and-finetune pipeline, which iteratively assigns pseudo labels for data then trains the feature extractor with the pseudo labels. In practice, since the ReID image data is generated from a distributed camera network, the correlation among images is usually diverse, heterogeneous, and complicated. Therefore, the relations are various, such as visual connections and camera connections, which causes the unreliable pseudo labels in unsupervised person ReID. To solve this issue, a hypergraph representation [16] is an appropriate tool to model the multi-modal and heterogeneous data correlation by means of a variety of hyperedges [10]. Due to the heterogeneous information in the metadata, the relationship among instances are varied from the different viewpoints. To address this issue, we propose three kinds of hypergraph construction techniques: “Global Clustering”, “Intra-camera Clustering”, and “Global KNN”. As illustrated in Figure 2, “Global Clustering” means performing DBSCAN on all data and then grouping the instances in a cluster as a hyperedge, this strategy aims to capture the global density-based mode in the data. “Intra-camera Clustering” considers the camera information and performs DBSCAN under an individual camera, this strategy concentrates on capture the camera-conditioned marginal density mode. “Global KNN” stands for building a hyperedge by connecting one vertex with its K nearest neighbors, this strategy focuses on local neighborhood to capture the smoothness locally. By means of merging several hyperedges created by different approaches, the hypergraph is able to perceive

the camera topology and model the heterogeneous data correlation across cameras. With this hypergraph, we can generate more reliable pseudo labels in learning process.

Given the generated pseudo labels, the ReID model could be finetuned iteratively. Several approaches related to mutual learning [3, 11, 44, 58] and memory-based contrastive loss [43, 68] are proposed to learn the robust feature representation with noisy labels. Although these proposed classification losses are verified to be effective, the end task such as average precision is not directly optimized in these approaches. To help address this issue, we propose a listwise loss combined with an instance-level memory, which provides a fine-grained supervision by directly optimize average precision in an approximate manner. Besides, we combine the proposed listwise loss and camera-aware contrastive loss as coarse-to-fine supervision for model updating.

Based on the motivation above, we propose a novel method termed **Metadata Guided Hypergraph (MGH)** to mutually guide the process of label refinement and feature learning. Specifically, we construct a heterogeneous hypergraph based on the metadata to generate pseudo labels, and utilize coarse-to-fine memory-based supervision to update the model. To achieve this, we first generate the noisy pseudo labels by clustering the visual feature representations of all unlabeled images. Then utilize hypergraph for label refinement. Specifically, we construct the hyperedges based on a joint similarity matrix [40] by considering visual information and spatio-temporal context simultaneously. Hyperedges are grouped to generate a hypergraph, which models the complicated high-order relationships among the data. Then, we perform label propagation on the hypergraph structure, which rectifies the label errors caused by the previous clustering algorithm. For model updating, the instance-level memory and camera-aware prototype memory are constructed to simultaneously capture local and global distribution. We propose to use a listwise loss based on the instance-level memory, which is combined with a camera-aware contrastive loss to provide coarse-to-fine supervision.

In summary, our main contributions are three-fold as follows:

- We propose a heterogeneous hypergraph to model the complicated data correlation among the metadata, which facilitates the unsupervised person ReID in the real-world scenario.
- We propose a novel unsupervised person ReID model named **MGH**, which consists of label generation with hypergraph and model updating through memory-based coarse-to-fine supervision.
- On three public person ReID benchmarks with readily available metadata, i.e. camera index and timestamp, our proposed method outperforms the state-of-the-art approaches.

2 RELATED WORK

2.1 Person ReID

Unsupervised Person ReID. Recent deep learning-based unsupervised person ReID and highly correlated unsupervised domain adaptive person ReID approaches could be classified into two camps: (1) distribution alignment, and (2) pseudo-label-based methods. For distribution alignment approaches, the purpose is to learn domain invariant feature representations. In [6, 17, 21, 28, 31, 62, 63,

66, 71], generative models such as a generative adversarial network (GAN) are exploited to achieve image-to-image translation from the source domain to the target domain and then use the generated images to train the model. Some other approaches [34] align the feature space by MMD loss. Current leading approaches perform label estimation and train the model accordingly. Such an operation is iteratively executed until the model converges. Fan *et al.* [7] and Song *et al.* [36] firstly utilize such pipeline for unsupervised person ReID. SSG [9] extends these methods by utilizing clustering on the part features and global features. BUC [25] and HTC [53] propose bottom-up clustering algorithm tailored for person ReID. Besides, in [38], memory-based multi-label classification loss named MMCL is proposed, which combines non-parametric classifier, multi-label classification, and single-label classification in a unified framework. Similarly, Lin *et al.* [27] use a soft label to represent instance similarity with custom distance metric for unsupervised person ReID. Furthermore, in [3, 8, 11, 54, 55, 58, 60], mutual learning combines the off-line hard pseudo label and on-line soft pseudo labels in an alternative training scheme.

Person ReID with Metadata. As mentioned above, there is a wealth of valuable meta information in the distributed camera network, such as camera index, timestamp, etc. Wang *et al.* [40] propose a joint metric considering spatio-temporal information and appearance similarity for supervised person ReID. Lv *et al.* [33] propose an unsupervised incremental learning scheme named TFusion, which builds up a Bayesian fusion model to combine the spatio-temporal pattern with visual features. Liao *et al.* [24] propose an effective post-processing strategy named TLift to enhance the retrieval stability of ReID model. In [43, 48], camera-aware learning is proposed to simultaneously consider intra-camera consistency and inter-camera matching.

2.2 Hypergraph

Graphs have been widely explored in computer vision tasks, such as image classification [5], image retrieval [16], person ReID [50], segmentation [18] etc. While the conventional graph is validated effective in the recent approaches, it could only model the pairwise relationships, which is hard to extend to the complicated data structure. Therefore, hypergraph [70] is introduced to model the high-order data correlation. An *et al.* [1] utilize hypergraph to learn the weight for multi-modal feature fusion in person ReID. Besides, Yan *et al.* [52] leverage hypergraph neural network to learn the multi-granular feature representation for video-based person ReID. Different from these methods, we utilize hypergraph for label refinery. By propagating residual label error on the hypergraph and smoothing the corrected labels, we obtain the more reliable labels.

2.3 Metric Learning

In the computer vision community, metric learning [19, 29, 42, 59] is widely used for learning discriminative feature representations. In face recognition, classification loss such as margin-based cross entropy loss [39] is widely explored. In [14], triplet loss is widely studied for person ReID, and recent approaches [32, 41] for person ReID commonly combine cross entropy loss and triplet loss to train the ReID model. However, these objective functions could not directly optimize the ranking tasks. In image retrieval, the listwise loss

is widely explored to optimize the mean average precision (mAP). Inspired by the recent works [2, 45], we develop a memory-based listwise loss to directly optimize AP in an approximate manner.

3 METHODOLOGY

Unsupervised person ReID aims to adapt the pretrained model to the target domain, which contains plenty of images without annotations but rich metadata such as camera index and timestamp. In this paper, we apply metadata including camera index and timestamp to improve the performance of ReID model.

Given an unlabeled target dataset $\mathcal{D} = \{(x_i, c_i, t_i)\}_{i=1}^N$ with N images, where x_i is i -th image, c_i, t_i are its camera index and timestamp respectively. We adopt a hypergraph $G = (V, E, w)$ to encode the complex relationships, where $V, E,$ and w are vertex set, hyperedge set, and hyperedge weights, respectively. The hyperedge is built based on the similarity matrix \mathcal{J} , where $\mathcal{J}(i, j)$ measures the pairwise similarity for vertex i and j . With the hypergraph, we perform label propagation to generate robust pseudo labels. Furthermore, we could fine-tune the ReID model f_θ with parameters θ , which is initialized by pretrained model. Table 1 shows the main notations used here in after.

Symbol	Brief Description
x, c, t	image, camera index, timestamp
\mathcal{D}	dataset
N	number of images
f_θ	ReID model
\mathcal{J}	joint similarity matrix
G, V, E	hypergraph, vertices, hyperedge
w, H	hypergraph weight, incidence matrix
$d(v), \delta(e)$	vertex, hyperedge degree
D_v, D_e	vertex, hyperedge degree matrix
W	hyperedge weight matrix
S_v, S_{st}	visual and spatio-temporal similarity matrix
A	hypergraph adjacency matrix
Δ_t	time interval in histogram
N_c	number of cluster
n_{c_i, c_j}^b	number of image pairs with the same labels
\mathcal{B}	histogram
y, \mathcal{Y}	pseudo label
$\hat{\mathcal{Y}}$	corrected pseudo label
$\mathcal{E}_r, \mathcal{E}_u$	error matrix
$\mathbb{S}_r, \mathbb{S}_u$	instance set
\mathcal{Y}_{soft}	soft pseudo label

Table 1: Notation table.

3.1 Meta Hypergraph Construction

Meta Hyperedge Construction

Metadata information is crucial for modeling the high-order heterogeneous data correlation in a distributed camera network, and such data correlation plays a vital role in distinguishing hard ReID matchings in the real-world scenario. To well model the diverse, heterogeneous, and complicated correlation, hypergraph is an appropriate tool by utilizing flexible hyperedges. How to define the

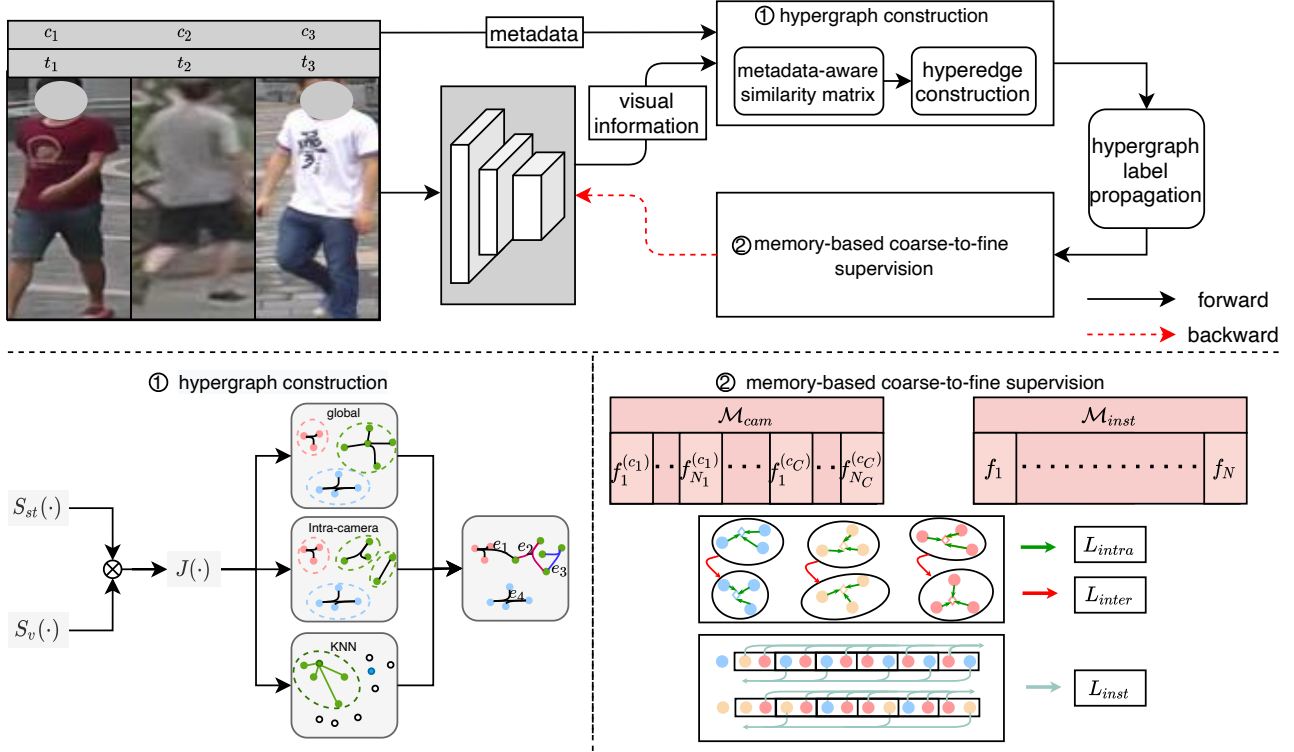


Figure 3: Diagram of our proposed method MGH. Our proposed method is a pseudo-label-based method, which follows the clustering-and-finetune pipeline that iteratively assigns the pseudo label for data and then finetunes the feature extractor until the training converges.

hypergraph directly affects the effectiveness of the data correlation modeling. As illustrated in Figure 3, we propose three kinds of hyperedge construction approaches, termed “Global Clustering”, “Intra-camera Clustering”, and “Global KNN” respectively, the different hyperedges could complement each other to encode complicate high-order data correlations.

- **Global Clustering**: we use clustering to directly group all vertices into clusters, and connects the vertices in each cluster by a hyperedge.
- **Intra-camera Clustering**: with the camera information, all vertices could be separated by the different camera, then we perform clustering to group vertex in each camera.
- **Global KNN**: in this method, we build a hyperedge by connecting one vertex with its K nearest neighbors.

By merging several hyperedges created by different approaches, the hypergraph is able to perceive the camera topology and model the heterogeneous data correlation across cameras. Besides, the weight of each hyperedge can be measured by:

$$w(e) = \sum_{i,j \in e} \exp\left(\frac{\mathcal{J}(i,j)^2}{\sigma^2}\right), \quad (1)$$

where (i, j) denote a pair of vertices in the hyperedge e , and σ is the medium value of the similarity of all vertex pairs. Then the hypergraph could be represented by an incidence matrix $H \in$

$$\mathbb{R}^{|V| \times |E|}:$$

$$H(v_i, e_j) = \begin{cases} \mathcal{J}(j, i) & \text{if } v_i \in e_j \\ 0 & \text{otherwise.} \end{cases} \quad (2)$$

According to this definition, higher weighted hyperedge includes the vertices with higher inner similarity. Besides, the vertex degree and hyperedge degree are defined as $d(v) = \sum_{e \in E} w(e)H(v, e)$ and $\delta(e) = \sum_{v \in V} H(v, e)$, respectively. The corresponding diagonal matrices of the vertex degree, the hyperedge degree, and hyperedge weight are D_v , D_e , and W , respectively. Then we define the hypergraph adjacency matrix as follows:

$$A = HWD_e^{-1}H^\top. \quad (3)$$

With the adjacency matrix, we could perform label propagation to correct the label noise.

Metadata-aware Similarity Matrix

To construct the hyperedges, we present the calculation of joint similarity matrix \mathcal{J} . As shown in Figure 3, by jointly considering the visual similarity and spatio-temporal similarity, the joint pairwise similarity is

$$\mathcal{J}(i, j) = \frac{1}{1 + \lambda_0 e^{-\gamma_0 S_v(i, j)}} \cdot \frac{1}{1 + \lambda_1 e^{-\gamma_1 S_{st}(i, j)}}, \quad (4)$$

where $S_v(i, j)$ and $S_{st}(i, j)$ are the visual and spatio-temporal similarity of the images x_i and x_j , respectively, and $S_v(i, j)$ is cosine similarity in our implementation.

To obtain the spatio-temporal similarity, we first perform clustering based on features $\{f_\theta(\mathbf{x}_i)\}_{i=1}^N$ and get the noisy pseudo labels $\mathcal{Y} = \{y_i\}_{i=1}^N$, where $y_i \in \mathbb{R}^{N_c}$ and N_c is the number of clusters. With the pseudo labels, we could build the spatio-temporal pattern through the spatio-temporal distribution, which is represented as the normalized histograms:

$$\mathcal{B}(\mathbb{I}(y_i, y_j) | c_i, c_j, b) = \frac{n_{c_i, c_j}^b}{\sum_l n_{c_i, c_j}^l}, \quad (5)$$

where b , c , and $\mathbb{I}(\cdot)$ are the index of histogram bins, the camera index, and indicator function, respectively. And n_{c_i, c_j}^b is the number of image pairs with the same labels whose time differences are in the scale of $((b-1)\Delta_t, b\Delta_t)$. Based on this spatio-temporal distribution, we can estimate the spatio-temporal consistency of two images (\mathbf{x}_i, c_i, t_i) and (\mathbf{x}_j, c_j, t_j) as follows:

$$\mathcal{S}_{st}(i, j) = \mathcal{B}(\mathbb{I}(y_i, y_j) | c_i, c_j, \lfloor \frac{|t_i - t_j|}{\Delta_t} \rfloor), \quad (6)$$

where $\lfloor \cdot \rfloor$ is round function.

3.2 Meta Hypergraph Guided Label Generation

In unsupervised person ReID, the pseudo-label-based methods generally follow the pipeline that alternatively assigns pseudos label and finetune the feature extractor until the training converges. Given the extracted feature representations, the first step is to generate reliable pseudo labels, which means grouping the same identities into an individual cluster. In the previous methods, several clustering algorithms such as K-Means and DBSCAN [13, 26, 36] have been explored. The existing methods generally perform label generation based on the pairwise visual relationships, which neglect the auxiliary spatio-temporal constraints. Here we adopt a hypergraph to model the diverse and heterogeneous data structure, and then refine the noisy pseudo label by either correcting the wrong labels or smoothing the noisy labels on a hypergraph.

Label propagation [20, 22, 56, 69] has been adopted to smooth the label prediction. Following the motivation that label prediction is highly correlated along edges in the graph, we perform label propagation on the hypergraph for label refinement.

Specifically, we first select 4 instances each cluster to be the most reliable instances \mathbb{S}_r , and the reliable prediction \mathcal{Y}_r , the extra unreliable instances are defined as \mathbb{S}_u . Then we could define error matrix \mathcal{E} as follows:

$$\mathcal{E}_r = \mathcal{Y} - \mathcal{Y}_r, \mathcal{E}_u = 0, \quad (7)$$

where $\mathcal{Y}_r \in \mathbb{R}^{N \times N_c}$ consists of one-hot vector on the selected reliable predictions and zero elsewhere, \mathcal{Y} is the initial noise label, and \mathcal{E}_u is the error matrix for unreliable instances. Then we perform iterative label propagation upon the hypergraph following the scaled fixed diffusion method proposed by [15], which iteratively propagates residual error as follows:

$$\mathcal{E}_u^{(t+1)} = \alpha_1 [D^{-1/2} A D^{-1/2} \mathcal{E}^{(t)}]_u, \quad (8)$$

where $[\cdot]_u$ means selecting unreliable entries in the error matrix. We fix reliable prediction $\mathcal{E}_r^{(t)} = \mathcal{E}_r$ until converging to $\hat{\mathcal{E}}$, and obtain the corrected label prediction $\hat{\mathcal{Y}}_r = \mathcal{Y}_r + s\hat{\mathcal{E}}$, where s is a

Algorithm 1: Meta Hypergraph Guided Network

Input: Unlabeled dataset $D = \{(\mathbf{x}_i, c_i, t_i)\}_{i=1}^N$, pretrained ReID model f_θ , number of epochs *Epoch*, number of iterations in each epoch *Iters*.

Output: Finetuned ReID model \hat{f}_θ .

```

1 while  $1 \leq i \leq Epoch$  do
  /* Meta Hypergraph Guided Label Generation */
2   Construct joint similarity matrix based on Equ. 4;
3   Construct incidence matrix  $H$  based on Equ. 2;
4   Generate pseudo label  $\hat{\mathcal{Y}}$  based on Equ. 8 and Equ. 9;
  /* Memory-based Coarse-to-fine Supervision */
5   Construct instance-level memory  $M^{inst}$  and
   camera-aware prototype memory  $M^{cam}$ ;
6   for  $j = 1:Iters$  do
7     Calculate entire loss by Equ. 14;
8     Update ReID model  $f_\theta$ ;
9   end
10 end
11 Output finetuned ReID model  $\hat{f}_\theta$ .

```

scale coefficient. Further, we smooth the prediction by iterative label propagation as follows:

$$\mathcal{Y}^{(t+1)} = (1 - \alpha_2)\mathcal{Y} + \alpha_2 D^{-1} A \mathcal{Y}^{(t)}. \quad (9)$$

The iteratively updated prediction \mathcal{Y}^t converges to final prediction.

3.3 Memory-based Coarse-to-fine Supervision

After label correction with hypergraph label propagation, we obtain the reliable labels $\hat{\mathcal{Y}}$. We propose to utilize memory-based coarse-to-fine supervision to guide the model training. More specifically, we build two memory banks: instance-level memory \mathcal{M}^{inst} and camera-aware prototype memory \mathcal{M}^{cam} , which are initialized with extracted features every epoch and updated in a moving average manner during the training process.

In the instance-level memory, all feature representations are stored and updated in the training process. Based on the instance-level memory bank, we adopt a listwise loss named Smooth-AP [2] to directly optimize mean average precision. Different from Smooth-AP that treats the in-batch images as the gallery, we compute the relevance score between query and features in the memory bank. This makes more hard negative samples participate in loss calculation. For a query image \mathbf{x}_q , the smoothed average precision is defined as:

$$AP_q \approx \frac{1}{|\mathbb{S}_P|} \sum_{i \in \mathbb{S}_P} \frac{1 + \sum_{j \in \mathbb{S}_P} \mathcal{G}(q, j)}{1 + \sum_{j \in \mathbb{S}_P} \mathcal{G}(q, j) + \sum_{j \in \mathbb{S}_N} \mathcal{G}(q, j)}, \quad (10)$$

$$\mathcal{G}(q, j) = \frac{1}{1 + e^{-f_\theta(\mathbf{x}_q)^\top \mathcal{M}_j^{inst}}},$$

where \mathbb{S}_P and \mathbb{S}_N are positive set and negative set for query q , which are consists of 1000 instances with the highest similarity to query. Then L_{inst} is defined as:

$$L_{inst} = \frac{1}{N} \sum_{q=1}^N (1 - AP_q). \quad (11)$$

Because of the variation between different scenes, intra-camera matching is more robust than inter-camera matching, we build camera-aware prototype memory to store the camera-aware prototypes, which depicts more precise camera-aware data distribution. For instance, the identity under different cameras has different prototypes. Moreover, we adopt weighted intra-camera loss and inter-camera loss to keep the intra-camera discrimination and encourage inter-camera matching, which is formulated as follows:

$$\begin{aligned} \mathcal{L}_{intra} &= -\sum_{c=1}^C \frac{1}{N_c} \sum_{x_i \in \mathbb{S}_c} \sum_{k=1}^{Z_c} \hat{Y}_{soft}(i, k) \log \frac{\phi(i, k)}{\sum_{k=1}^{Z_c} \phi(i, k)}, \\ \mathcal{L}_{inter} &= -\sum_{i=1}^{N'} \frac{1}{|\mathcal{P}|} \sum_{p \in \mathcal{P}} \log \frac{\phi(i, p)}{\sum_{u \in \mathcal{P}} \phi(i, u) + \sum_{q \in \mathcal{Q}} \phi(i, q)}, \end{aligned} \quad (12)$$

where $\phi(i, k) = \exp(f_{\theta}(x_i)^T M_j^{cam}/\tau)$, \mathbb{S}_c is the dataset of the c -th camera, Z_c is the number of identity in \mathbb{S}_c , and \mathcal{P} , \mathcal{Q} denote the index sets of positive and negative prototypes for x_i , and \hat{Y}_{soft} is soft label calculated based on \mathcal{J} and \hat{Y} as follows:

$$\hat{Y}_{soft}(i, n_c) = \sum_{m \in M} \frac{\mathcal{J}(i, m)}{|M|}, M = \{m | \mathcal{Y}(m, n_c) = 1\}, \quad (13)$$

where $n_c \in [1, 2, \dots, N_c]$ is the class index. For training the network, we formulate the entire loss function as follows:

$$\mathcal{L} = \lambda_1 \mathcal{L}_{intra}(\mathcal{X}, \hat{Y}) + \lambda_2 \mathcal{L}_{inter}(\mathcal{X}, \hat{Y}) + \lambda_3 \mathcal{L}_{inst}(\mathcal{X}, \hat{Y}), \quad (14)$$

where \mathcal{L}_{intra} , \mathcal{L}_{inter} , and \mathcal{L}_{inst} are weighted intra-camera loss, inter-camera loss, and instance loss, respectively. We summarize the overall algorithm is summarized in Algorithm 1.

4 EXPERIMENTS

4.1 Experiment setting

Dataset and Protocol. In this paper, we evaluate the performance on three public benchmarks Market1501 [61], DukeMTMC [35, 63], and MSMT17 [47]. We follow the standard evaluation setting in the previous methods to evaluate our proposed method, cumulative matching characteristic (CMC) at Rank-1, Rank-5, Rank-10 and mean average precision (mAP) are reported for comparison.

Implementation Details. We follow same settings as [32] for backbone, which sets the stride of the last residual block as 1 and adds a batch normalization layer. In label generation, we set Δ_t to 100 frames for spatio-temporal distribution, and we use jaccard distance metric with k-reciprocal nearest neighbors [64] for clustering, α_1 and α_2 are 0.99 and 0.9 respectively. For memory-based supervision, the most hyperparameter setting follows [43], the instance-level memory is updated by replacing the corresponding features, and camera-aware prototype memory is updated with a moving average rate as 0.2, temperature τ is set as 0.07, loss weight $\lambda_1, \lambda_2, \lambda_3$ are 1, 1, and 10 separately. In the training stage, we adopt random erasing [65], random flip, cropping as data augmentation strategy, and the images are resized to 256×128 before processing. We set the mini-batch as 32 and use Adam optimizer to optimize the network for 50 epochs, and there are 400 iterations in each epoch. The initial learning rate is $3.5e-4$ and divided by 10 every 20 epochs, weight decay is set to $3e-4$. In the first 5 epochs, only a weighted intra-camera loss is calculated. In addition, we set

Model	Market		DukeMTMC	
	R1	mAP	R1	mAP
evaluation of individual components				
CAP	91.4	79.2	81.1	67.3
CAP*	91.5	79.7	81.5	67.3
Sbase	92.3	80.8	82.2	68.7
Sbase w/ \mathcal{L}_{inst}	92.7	81.3	83.1	69.3
Sbase w/ HG	92.7	81.8	83.3	70
Sbase w/ \mathcal{L}_{inst}+HG (MGH)	93.2	81.7	83.6	70.2
impact of hyperparameter λ_3				
$\lambda_3=0$	92.3	80.8	82.2	68.7
$\lambda_3=1$	92.1	81.3	82.5	69.3
$\lambda_3=10$	92.7	81.3	83.1	69.3
$\lambda_3=100$	92.2	81.2	83	69.1

Table 2: (1) Evaluation of individual component. Based on CAP [43], we propose a strong baseline denoted Sbase with weighted intra-camera loss. \mathcal{L}_{inst} short for instance-level memory based listwise loss. HG means hypergraph label correction. Our final model combines \mathcal{L}_{inst} and HG named MGH. (2) The Impact of Hyperparameter λ_3 . We compare different value of λ_3 .

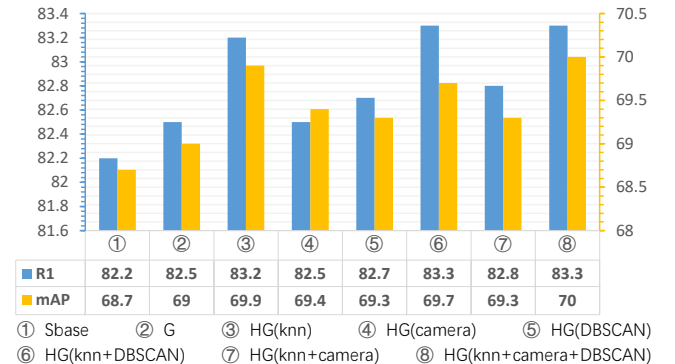


Figure 4: Ablation study on the effectiveness of hypergraph construction on DukeMTMC. Base on Sbase, we investigate different ways to construct hypergraph. KNN is constructing hypergraph with k nearest neighbors, DBSCAN means constructing hypergraph with cluster results of DBSCAN. camera means camera-aware DBSCAN which performs DBSCAN on each camera. Experimental results on Market1501 could be found in the supplementary material.

$K = 10, 20, 30, 40, 50$ in “Global KNN”. And we propose a strong baseline model denoted **Sbase** based on CAP [43], which modifies the original intra-camera loss to weighted intra-camera loss and sets the loss weight for inter-camera loss as 1.

4.2 Ablation Studies

Evaluation of Individual Components. To investigate the effectiveness of individual components in our proposed MGH, e.g. \mathcal{L}_{inst} and hypergraph label correction. Here we use Market1501

Method	Reference	Market1501					DukeMTMC				
		source	R1	R5	R10	mAP	source	R1	R5	R10	mAP
Unsupervised person ReID											
BUC [25]	AAAI19	None	66.2	79.6	84.5	38.3	None	47.4	62.6	68.4	27.5
SpCL [12]	NeurIPS20	None	87.7	95.2	96.9	72.6	None	81.2	90.3	92.2	65.3
HCT [53]	CVPR20	None	80.0	91.6	95.2	56.4	None	69.6	83.4	87.4	50.7
MMCL [38]	CVPR20	None	80.3	89.4	92.3	45.5	None	65.2	75.9	80.0	40.2
UDA person ReID											
PUL [7]	TOMM18	Duke	45.5	60.7	66.7	20.5	Market	30.0	43.4	48.5	16.4
SPGAN+LMP [6]	CVPR18	Duke	58.1	76.0	82.7	26.9	Market	46.9	62.6	68.5	26.4
SSG [9]	ICCV19	Duke	80.0	90.0	92.4	58.3	Market	73.0	80.6	83.2	53.4
UDAP [36]	PR20	Duke	75.8	89.5	93.2	53.7	Market	68.4	80.1	83.5	49.0
MMCL [38]	CVPR20	Duke	84.4	92.8	95.0	60.4	Market	72.4	82.9	85.0	51.4
MMT [11]	ICLR20	Duke	89.5	96.0	97.6	73.8	Market	76.3	87.7	91.2	62.3
SpCL [12]	NeurIPS20	Duke	90.3	96.2	97.7	76.7	Market	82.9	90.1	92.5	68.8
MEB-Net [55]	ECCV20	Duke	89.9	96.0	97.5	76.0	Market	79.6	88.3	92.2	66.1
AD-Cluster [54]	CVPR20	Duke	86.7	94.4	96.5	68.3	Market	72.6	82.5	85.5	54.1
DIM+GLO [30]	MM20	Duke	88.3	94.7	96.3	65.1	Market	76.2	85.7	88.5	58.3
UNRN [60]	AAAI21	Duke	91.9	96.1	97.8	78.1	Market	82.0	90.7	93.5	69.1
Unsupervised person ReID with meta information											
JVTC+ [23]	ECCV20	None	79.5	89.2	91.9	47.5	None	74.6	82.9	85.3	50.7
ECN++ [68]	TPAMI20	None	84.1	92.8	95.4	63.8	None	74.0	83.7	87.4	54.4
CAP [43]	AAAI21	None	91.4	96.3	97.7	79.2	None	81.1	89.3	91.8	67.3
TFusion [33]	CVPR18	CUHK01	60.8	74.4	79.3	-	-	-	-	-	-
UGA [49]	ICCV19	Tracklet	87.2	-	-	70.3	Tracklet	75.0	-	-	53.3
JVTC+ [23]	ECCV20	Duke	86.8	95.2	97.1	67.2	Market	80.4	89.9	92.2	66.5
MGH(Ours)	-	None	93.2	96.8	98.1	81.7	None	83.7	92.1	93.7	70.2
MGH+(Ours)	-	None	95.5	98.2	98.7	84.0	None	91.0	94.2	95.3	77.2

Table 3: Comparison with state-of-the-art methods on Market1501 and DukeMTMC. We compare our method to the state-of-the-art methods for unsupervised person ReID, UDA person ReID, and unsupervised person ReID with meta information. The top-3 best results are highlighted with red, green, and blue respectively. MGH+ uses joint similarity to compute the query-gallery similarity.

and DukeMTMC to perform the ablation study, the experimental results are listed in Table 2. It is apparent that **Sbase** with weighted intra-camera loss is better than CAP. To be specific, Rank-1 and mAP are improved from 91.5%/79.7% to 92.3%/80.8% on Market1501 and from 81.5%/67.3% to 82.2%/68.7% on DukeMTMC. By combining \mathcal{L}_{inst} with **Sbase**, we could achieve Rank-1/mAP 92.7%/81.3% and 83.1%/69.3% on Market1501 and DukeMTMC, which indicates the effectiveness of listwise loss based on instance-level memory. In addition, hypergraph label correction could improve Rank-1/mAP by 0.4%/1.0% and 1.1%/1.3% on these two datasets. Overall, the final model (MGH) could significantly boost the performance by 0.9%, 0.9% mAP and 1.4%, 1.5% Rank-1 respectively compared with **Sbase**.

The Impact of Hyperparameter λ_3 . The parameter λ_3 in Equation 14 is crucial to the final performance. In Table 2, we compare the different values of λ_3 . When $\lambda_3 = 0$, the method is exactly **Sbase** that only uses weighted intra-camera loss and inter-camera loss. It is clear that when utilizing instance-memory-based listwise loss, our approach could improve the **Sbase** at all values. In our experiments, when λ_3 is set to 10, we achieve the highest results. Thus, we use $\lambda_3 = 10$ in our final model.

Effectiveness of Hypergraph Construction. As mentioned in Section 3.2, how to construct hypergraph is important for modeling data correlation, so we investigate the different hypergraph construction methods. As shown in Figure 4, we utilize K nearest neighbor (KNN), DBSCAN, and camera-aware DBSCAN (denoted as camera, perform DBSCAN on each camera) to construct hypergraph. Except for the hypergraph, we also present the results of the conventional graph (**Sbase** w/ G), it also improve the performance compared with **Sbase**. While the high-order information could not be well modeled in the conventional graph, so the improvement is minor. For KNN, each vertex is treated as the centroid to find the K nearest neighbors, and the neighbors are grouped to generate a hyperedge. For DBSCAN and camera-aware DBSCAN, each cluster is a hyperedge in the hypergraph. The reason why HG(KNN) is superior to HG(KNN+Camera) maybe is the noisy and unstable pseudo labels in “Global Clustering” and “Intra-camera Clustering”. In our experiments, several hyperedge construction strategies are adopted, we find multi-scale KNN is most effective and adopting “Global Clustering” and “Intra-camera Clustering” in hypergraph construction is not stable. From the experimental results, we find combining these three hypergraph construction strategies yields

the best performance. Thus, we use HG(KNN+camera+DBSCAN) to build a hypergraph in our proposed method.

According to the experimental results, in our opinion, constructing hypergraph should follow three criterions in unsupervised person ReID: 1) Complementary. different strategies should reinforce each other. 2) Accurate and stable. The information for hypergraph construction should be accurate for modelling the data correlation. 3) Multi-scale. Our experimental results indicate that multi-scale local information is effective.

4.3 Comparison with State-of-the-art Methods

In this section, we compare our proposed MGH with the state-of-the-art unsupervised and domain adaptive person ReID approaches on Market1501, DukeMTMC, and MSMT17 datasets.

Comparison on Market1501 and DukeMTMC. We compare our proposed method with the state-of-the-art unsupervised learning approaches, including 15 approaches without meta information [6, 7, 9, 11, 12, 25, 27, 36, 38, 46, 53–55, 57, 60], and 5 approaches with meta information [23, 33, 43, 49, 67, 68]. Table 3 shows the results on Market1501 and DukeMTMC, we observe that our proposed method outperforms all the previous approaches. Compared with the best unsupervised ReID approach SpCL [12], MGH outperforms by a large margin. Even compared with the UDA methods which exploits an external labeled data, we still have a better result. In comparison with the best UDA methods UNRN [60], although we only use data in the target domain, we still obtain an improvement of 1.3% Rank-1 and 3.6% on Market1501, 1.7% Rank-1 and 1.1% mAP on DukeMTMC. When only target dataset is accessible, our method surpasses the best method CAP [43] by 1.8% Rank-1 and 2.5% mAP on Market1501, 2.6% Rank-1 and 2.9% mAP on DukeMTMC. MGH+ could improve the performance further by using joint similarity to compute the query-gallery similarity in testing stage.

Comparison on MSMT17. On MSMT17, we compare our MGH with several methods and report the results on Table 4. The results obtained by MGH are 70.2%/40.6% on Rank-1/mAP accuracy, which exceeds the second best method CAP by 2.8%/3.7% on Rank-1/mAP. Compared with the supervised ReID method PCB, our method has a better result. This demonstrates the effectiveness of our proposed MGH on the large scale dataset.

Comparison with Supervised Approaches. We further present the comparison with the supervised counterpart. As shown in Table 5, our proposed unsupervised method MGH even outperforms PCB, which is trained with labeled information. And the gap with the state-of-the-art supervised method ABD-Net has been mitigated on three benchmarks. By further using joint similarity in testing stage, MGH+ can greatly narrow down the margin between ABD-Net.

5 CONCLUSION

This paper tackles the unsupervised person Re-ID by jointly considering the rich auxiliary meta information attached with the captured images in the distributed camera network. By constructing hypergraphs, we model the high-order data correlation and encode the multi-modal information, then a label correction approach is utilized to refine the noisy pseudo labels. Furthermore, to directly optimize AP, we propose a memory-based listwise loss,

Method	MSMT17				
	source	R1	R5	R10	mAP
Unsupervised person ReID					
SpCL [12]	None	42.3	55.6	61.2	19.1
MMCL [38]	None	35.4	44.8	49.8	11.2
UDA person ReID					
MMCL [38]	Market	40.8	51.8	56.7	15.1
MMT [11]	Market	50.1	63.5	69.3	24.0
SpCL [12]	Market	51.6	64.3	69.7	25.4
DIM+GLO [30]	Market	49.7	-	66.1	20.7
UNRN [60]	Market	52.4	64.7	69.7	25.3
MMCL [38]	Duke	43.6	54.3	58.9	16.2
MMT [11]	Duke	52.9	66.3	71.3	25.1
SpCL [12]	Duke	53.1	65.8	70.5	26.5
DIM+GLO [30]	Duke	56.5	-	70.0	24.4
UNRN [60]	Duke	54.9	67.3	70.6	26.2
Unsupervised person ReID with meta information					
UGA [49]	Tacklet	49.5	-	-	21.7
CAP [43]	None	67.4	78.0	81.4	36.9
ECN++ [68]	Market	40.4	53.1	58.7	15.2
JVTC+ [23]	Market	48.6	65.3	68.2	25.1
ECN++ [68]	Duke	42.5	55.9	61.5	16.0
JVTC+ [23]	Duke	52.9	70.5	75.9	27.5
MGH(Ours)	None	70.2	81.2	84.5	40.6
MGH+(Ours)	None	75.2	83.9	86.7	43.6

Table 4: Comparison with state-of-the-art methods on MSMT17. The top-3 best results are highlighted with red, green, and blue respectively. MGH+ uses joint similarity to compute the query-gallery similarity.

Method	Market1501		DukeMTMC		MSMT17	
	R1	mAP	R1	mAP	R1	mAP
PCB [37]	93.8	81.6	83.3	69.2	68.2	40.4
BoT [32]	94.5	85.9	86.4	76.4	74.1	50.2
ABD-Net [4]	95.6	88.3	89	78.6	82.3	60.8
MGH	93.2	81.7	83.7	70.2	70.2	40.6
MGH+	95.5	84	91	77.2	75.2	43.6

Table 5: Comparison with supervised person ReID methods on three benchmarks.

which stores the instance features in the memory bank, and used as the gallery in the training stage. Finally, to bridge the gap between experimental settings and real-world ReID tasks, we validate the effectiveness of our method on three widely used benchmarks and show our proposed MGH achieves a significant improvement compared with the previous approaches.

ACKNOWLEDGMENTS

This work is supported in part by National Key Research and Development Program of China under Grant 2020AAA0107400, Zhejiang Provincial Natural Science Foundation of China under Grant LR19F020004, key scientific technological innovation research project by Ministry of Education, and National Natural Science Foundation of China under Grant U20A20222, and Collaborative Innovation Center of Artificial Intelligence by MOE and Zhejiang Provincial Government (ZJU).

REFERENCES

- [1] Le An, Xiaojing Chen, Songfan Yang, and Xuelong Li. 2016. Person re-identification by multi-hypergraph fusion. *IEEE Trans. Neural Netw. Learn. Sys.* 28, 11 (2016), 2763–2774.
- [2] Andrew Brown, Weidi Xie, Vicky Kalogeiton, and Andrew Zisserman. 2020. Smooth-AP: Smoothing the path towards large-scale image retrieval. In *Proc. ECCV*. Springer, 677–694.
- [3] Hao Chen, Benoit Lagadec, and Francois Bremond. 2021. Enhancing Diversity in Teacher-Student Networks via Asymmetric branches for Unsupervised Person Re-identification. In *Proc. IEEE ICCV*. 1–10.
- [4] Tianlong Chen, Shaojin Ding, Jingyi Xie, Ye Yuan, Wuyang Chen, Yang Yang, Zhou Ren, and Zhangyang Wang. 2019. Abd-net: Attentive but diverse person re-identification. In *Proc. IEEE ICCV*. 8351–8361.
- [5] Zhao-Min Chen, Xiu-Shen Wei, Peng Wang, and Yanwen Guo. 2019. Multi-label image recognition with graph convolutional networks. In *Proc. IEEE Conf. CVPR*. 5177–5186.
- [6] Weijian Deng, Liang Zheng, Qixiang Ye, Guoliang Kang, Yi Yang, and Jianbin Jiao. 2018. Image-image domain adaptation with preserved self-similarity and domain-dissimilarity for person re-identification. In *Proc. IEEE Conf. CVPR*. 994–1003.
- [7] Hehe Fan, Liang Zheng, Chenggang Yan, and Yi Yang. 2018. Unsupervised person re-identification: Clustering and fine-tuning. *ACM Trans. on Multimedia* 14, 4 (2018), 1–18.
- [8] Hao Feng, Minghao Chen, Jinming Hu, Dong Shen, Haifeng Liu, and Deng Cai. 2021. Complementary Pseudo Labels For Unsupervised Domain Adaptation On Person Re-identification. *IEEE Trans. Image Process.* 30 (2021), 2898–2907.
- [9] Yang Fu, Yunchao Wei, Guanshuo Wang, Yuqian Zhou, Honghui Shi, and Thomas S Huang. 2019. Self-similarity grouping: A simple unsupervised cross domain adaptation approach for person re-identification. In *Proc. IEEE ICCV*. 6112–6121.
- [10] Yue Gao, Zizhao Zhang, Haojie Lin, Xibin Zhao, Shaoyi Du, and Changqing Zou. 2020. Hypergraph Learning: Methods and Practices. *IEEE Trans. Pattern Anal. and Mach. Intell.* (2020).
- [11] Yixiao Ge, Dapeng Chen, and Hongsheng Li. 2020. Mutual mean-teaching: Pseudo label refinery for unsupervised domain adaptation on person re-identification. In *Proc. ICLR*.
- [12] Yixiao Ge, Dapeng Chen, Feng Zhu, Rui Zhao, and Hongsheng Li. 2020. Self-paced contrastive learning with hybrid memory for domain adaptive object re-id. In *Proc. NeurIPS*.
- [13] Jean-Bastien Grill, Florian Strub, Florent Altché, Corentin Tallec, Pierre Richemond, Elena Buchatskaya, Carl Doersch, Bernardo Avila Pires, Zhaohan Guo, Mohammad Gheshlaghi Azar, Bilal Piot, koray kavukcuoglu, Remi Munos, and Michal Valko. 2020. Bootstrap Your Own Latent - A New Approach to Self-Supervised Learning. In *Proc. NeurIPS*, H. Larochelle, M. Ranzato, R. Hadsell, M. F. Balcan, and H. Lin (Eds.), Vol. 33. Curran Associates, Inc., 21271–21284. <https://proceedings.neurips.cc/paper/2020/file/f3ada80d5c4ee70142b17b8192b2958e-Paper.pdf>
- [14] Alexander Hermans, Lucas Beyer, and Bastian Leibe. 2017. In defense of the triplet loss for person re-identification. *arXiv preprint arXiv:1703.07737* (2017).
- [15] Qian Huang, Horace He, Abhay Singh, Ser-Nam Lim, and Austin R Benson. 2020. Combining Label Propagation and Simple Models Out-performs Graph Neural Networks. In *Proc. ICLR*.
- [16] Yuchi Huang, Qingshan Liu, Shaoting Zhang, and Dimitris N Metaxas. 2010. Image retrieval via probabilistic hypergraph ranking. In *Proc. IEEE Conf. CVPR*. IEEE, 3376–3383.
- [17] Yukun Huang, Zheng-Jun Zha, Xueyang Fu, Richang Hong, and Liang Li. 2020. Real-world person re-identification via degradation invariance learning. In *Proc. IEEE Conf. CVPR*. 14084–14094.
- [18] Wei Ji, Xi Li, Lina Wei, Fei Wu, and Yueting Zhuang. 2020. Context-aware graph label propagation network for saliency detection. *IEEE Trans. Image Process.* 29 (2020), 8177–8186.
- [19] Wei Ji, Xi Li, Fei Wu, Zhijie Pan, and Yueting Zhuang. 2019. Human-centric clothing segmentation via deformable semantic locality-preserving network. *IEEE Trans. Circ. Sys. Vid. Tech.* 30, 12 (2019), 4837–4848.
- [20] Junteng Jia and Austin R Benson. 2020. Residual correlation in graph neural network regression. In *Proc. ACM SIGKDD Int. Conf. Knowl. Dis. Data Min.* 588–598.
- [21] Xin Jin, Cuiling Lan, Wenjun Zeng, Zhibo Chen, and Li Zhang. 2020. Style normalization and restitution for generalizable person re-identification. In *Proc. IEEE Conf. CVPR*. 3143–3152.
- [22] Johannes Klicpera, Aleksandar Bojchevski, and Stephan Gunnemann. 2019. Combining Neural Networks with Personalized PageRank for Classification on Graphs. In *Proc. ICLR*. <https://openreview.net/forum?id=H1gL-2A9Ym>
- [23] Jianing Li and Shiliang Zhang. 2020. Joint Visual and Temporal Consistency for Unsupervised Domain Adaptive Person Re-Identification. In *Proc. ECCV*. Springer, 483–499.
- [24] Shengcai Liao and Ling Shao. 2020. Interpretable and Generalizable Person Re-Identification with Query-Adaptive Convolution and Temporal Lifting. In *Proc. ECCV*.
- [25] Yutian Lin, Xuanyi Dong, Liang Zheng, Yan Yan, and Yi Yang. 2019. A bottom-up clustering approach to unsupervised person re-identification. In *Proc. AAAI*, Vol. 33. 8738–8745.
- [26] Yutian Lin, Yu Wu, Chenggang Yan, Mingliang Xu, and Yi Yang. 2020. Unsupervised person re-identification via cross-camera similarity exploration. *IEEE Trans. Image Process.* 29 (2020), 5481–5490.
- [27] Yutian Lin, Lingxi Xie, Yu Wu, Chenggang Yan, and Qi Tian. 2020. Unsupervised person re-identification via softened similarity learning. In *Proc. IEEE Conf. CVPR*. 3390–3399.
- [28] Chong Liu, Xiaojun Chang, and Yi-Dong Shen. 2020. Unity style transfer for person re-identification. In *Proc. IEEE Conf. CVPR*. 6887–6896.
- [29] Tie-Yan Liu. 2011. Learning to rank for information retrieval. *Foundations and Trends in Information Retrieval* (2011).
- [30] Xiaobin Liu and Shiliang Zhang. 2020. Domain Adaptive Person Re-Identification via Coupling Optimization. In *Proc. ACM Multimedia*. 547–555.
- [31] Chuanchen Luo, Chunfeng Song, and Zhaoxing Zhang. 2020. Generalizing person re-identification by camera-aware invariance learning and cross-domain mixup. In *Proc. ECCV*, Vol. 2. Springer, 7.
- [32] Hao Luo, Youzhi Gu, Xingyu Liao, Shenqi Lai, and Wei Jiang. 2019. Bag of tricks and a strong baseline for deep person re-identification. In *Proc. IEEE Conf. CVPR Workshop*. 0–0.
- [33] Jianming Lv, Weihang Chen, Qing Li, and Can Yang. 2018. Unsupervised cross-dataset person re-identification by transfer learning of spatial-temporal patterns. In *Proc. IEEE Conf. CVPR*. 7948–7956.
- [34] Djibril Mekhazni, Amran Bhuiyan, George Ekladios, and Eric Granger. 2020. Unsupervised domain adaptation in the dissimilarity space for person re-identification. In *Proc. ECCV*. Springer, 159–174.
- [35] Ergys Ristani, Francesco Solera, Roger Zou, Rita Cucchiara, and Carlo Tomasi. 2016. Performance measures and a data set for multi-target, multi-camera tracking. In *Proc. ECCV*. Springer, 17–35.
- [36] Liangchen Song, Cheng Wang, Lefei Zhang, Bo Du, Qian Zhang, Chang Huang, and Xinggang Wang. 2020. Unsupervised domain adaptive re-identification: Theory and practice. *Pattern Recognition* 102 (2020), 107173.
- [37] Yifan Sun, Liang Zheng, Yi Yang, Qi Tian, and Shengjin Wang. 2018. Beyond part models: Person retrieval with refined part pooling (and a strong convolutional baseline). In *Proc. ECCV*. 480–496.
- [38] Dongkai Wang and Shiliang Zhang. 2020. Unsupervised person re-identification via multi-label classification. In *Proc. IEEE Conf. CVPR*. 10981–10990.
- [39] Feng Wang, Jian Cheng, Weiyang Liu, and Haijun Liu. 2018. Additive margin softmax for face verification. *IEEE Signal Processing Letters* 25, 7 (2018), 926–930.
- [40] Guangcong Wang, Jianhuang Lai, Peigen Huang, and Xiaohua Xie. 2019. Spatial-temporal person re-identification. In *Proc. AAAI*, Vol. 33. 8933–8940.
- [41] Guanshuo Wang, Yufeng Yuan, Xiong Chen, Jiwei Li, and Xi Zhou. 2018. Learning discriminative features with multiple granularities for person re-identification. In *Proc. ACM Multimedia*. 274–282.
- [42] Hui Wang, Hanbin Zhao, Xi Li, and Xu Tan. 2018. Progressive Blockwise Knowledge Distillation for Neural Network Acceleration. In *Proc. IJCAI*. 2769–2775.
- [43] Menglin Wang, Baisheng Lai, Jianqiang Huang, Xiaojin Gong, and Xian-Sheng Hua. 2021. Camera-aware Proxies for Unsupervised Person Re-Identification. In *Proc. AAAI*.
- [44] Wenhao Wang, Fang Zhao, Shengcai Liao, and Ling Shao. 2020. Attentive Wave-Block: Complementarity-enhanced Mutual Networks for Unsupervised Domain Adaptation in Person Re-identification. *arXiv preprint arXiv:2006.06525* (2020).
- [45] Xun Wang, Haozhi Zhang, Weilin Huang, and Matthew R Scott. 2020. Cross-batch memory for embedding learning. In *Proc. IEEE Conf. CVPR*. 6388–6397.
- [46] Zhongdao Wang, Jingwei Zhang, Liang Zheng, Yixuan Liu, Yifan Sun, Yali Li, and Shengjin Wang. 2020. CycAs: Self-supervised Cycle Association for Learning Re-identifiable Descriptions. In *Proc. ECCV*. Springer.
- [47] Longhui Wei, Shiliang Zhang, Wen Gao, and Qi Tian. 2018. Person transfer gan to bridge domain gap for person re-identification. In *Proc. IEEE Conf. CVPR*. 79–88.
- [48] Ancong Wu, Wei-Shi Zheng, and Jian-Huang Lai. 2019. Unsupervised person re-identification by camera-aware similarity consistency learning. In *Proc. IEEE ICCV*. 6922–6931.
- [49] Jinlin Wu, Yang Yang, Hao Liu, Shengcai Liao, Zhen Lei, and Stan Z Li. 2019. Unsupervised graph association for person re-identification. In *Proc. IEEE ICCV*. 8321–8330.
- [50] Yiming Wu, Omar El Farouk Bourahla, Xi Li, Fei Wu, Qi Tian, and Xue Zhou. 2020. Adaptive graph representation learning for video person re-identification. *IEEE Trans. Image Process.* 29 (2020), 8821–8830.
- [51] Qiaokang Xie, Wengang Zhou, Guo-Jun Qi, Qi Tian, and Houqiang Li. 2020. Progressive Unsupervised Person Re-identification by Tracklet Association with Spatio-Temporal Regularization. *IEEE Trans. Multimedia* (2020).
- [52] Yichao Yan, Jie Qin, Jiabin Chen, Li Liu, Fan Zhu, Ying Tai, and Ling Shao. 2020. Learning multi-granular hypergraphs for video-based person re-identification. In *Proc. IEEE Conf. CVPR*. 2899–2908.

- [53] Kaiwei Zeng, Munan Ning, Yaohua Wang, and Yang Guo. 2020. Hierarchical clustering with hard-batch triplet loss for person re-identification. In *Proc. IEEE Conf. CVPR*. 13657–13665.
- [54] Yunpeng Zhai, Shijian Lu, Qixiang Ye, Xuebo Shan, Jie Chen, Rongrong Ji, and Yonghong Tian. 2020. Ad-cluster: Augmented discriminative clustering for domain adaptive person re-identification. In *Proc. IEEE Conf. CVPR*. 9021–9030.
- [55] Yunpeng Zhai, Qixiang Ye, Shijian Lu, Mengxi Jia, Rongrong Ji, and Yonghong Tian. 2020. Multiple expert brainstorming for domain adaptive person re-identification. In *Proc. ECCV*. Springer.
- [56] Hao Zhang, Liangxiao Jiang, and Wenqiang Xu. 2019. Multiple Noisy Label Distribution Propagation for Crowdsourcing. In *Proc. IJCAI*. 1473–1479.
- [57] Xiao Zhang, Yixiao Ge, Yu Qiao, and Hongsheng Li. 2021. Refining Pseudo Labels with Clustering Consensus over Generations for Unsupervised Object Re-identification. In *Proc. IEEE Conf. CVPR*.
- [58] Fang Zhao, Shengcai Liao, Guo-Sen Xie, Jian Zhao, Kaihao Zhang, and Ling Shao. 2020. Unsupervised domain adaptation with noise resistible mutual-training for person re-identification. In *Proc. ECCV*. Springer, 526–544.
- [59] Hanbin Zhao, Xin Qin, Shihao Su, Zibo Lin, and Xi Li. 2021. When Video Classification Meets Incremental Classes. *arXiv preprint arXiv:2106.15827* (2021).
- [60] Kecheng Zheng, Cuiling Lan, Wenjun Zeng, Zhizheng Zhan, and Zheng-Jun Zha. 2021. Exploiting Sample Uncertainty for Domain Adaptive Person Re-Identification. In *Proc. AAAI*.
- [61] Liang Zheng, Liyue Shen, Lu Tian, Shengjin Wang, Jingdong Wang, and Qi Tian. 2015. Scalable person re-identification: A benchmark. In *Proc. IEEE ICCV*. 1116–1124.
- [62] Zhedong Zheng, Xiaodong Yang, Zhiding Yu, Liang Zheng, Yi Yang, and Jan Kautz. 2019. Joint discriminative and generative learning for person re-identification. In *Proc. IEEE Conf. CVPR*. 2138–2147.
- [63] Zhedong Zheng, Liang Zheng, and Yi Yang. 2017. Unlabeled samples generated by gan improve the person re-identification baseline in vitro. In *Proc. IEEE ICCV*. 3754–3762.
- [64] Zhun Zhong, Liang Zheng, Donglin Cao, and Shaozi Li. 2017. Re-ranking person re-identification with k-reciprocal encoding. In *Proc. IEEE Conf. CVPR*. 1318–1327.
- [65] Zhun Zhong, Liang Zheng, Guoliang Kang, Shaozi Li, and Yi Yang. 2020. Random erasing data augmentation. In *Proc. AAAI*, Vol. 34. 13001–13008.
- [66] Zhun Zhong, Liang Zheng, Shaozi Li, and Yi Yang. 2018. Generalizing a person retrieval model hetero-and homogeneously. In *Proc. ECCV*. 172–188.
- [67] Zhun Zhong, Liang Zheng, Zhiming Luo, Shaozi Li, and Yi Yang. 2019. Invariance matters: Exemplar memory for domain adaptive person re-identification. In *Proc. IEEE Conf. CVPR*. 598–607.
- [68] Zhun Zhong, Liang Zheng, Zhiming Luo, Shaozi Li, and Yi Yang. 2020. Learning to adapt invariance in memory for person re-identification. *IEEE Trans. Pattern Anal. and Mach. Intell.* (2020).
- [69] Dengyong Zhou, Olivier Bousquet, Thomas Navin Lal, Jason Weston, and Bernhard Schölkopf. 2004. Learning with local and global consistency. In *Proc. NeurIPS*. 321–328.
- [70] Dengyong Zhou, Jiayuan Huang, and Bernhard Schölkopf. 2006. Learning with hypergraphs: Clustering, classification, and embedding. In *Proc. NeurIPS*, Vol. 19. Citeseer, 1601–1608.
- [71] Yang Zou, Xiaodong Yang, Zhiding Yu, BVK Kumar, and Jan Kautz. 2020. Joint disentangling and adaptation for cross-domain person re-identification. In *Proc. ECCV*.